

Characterising resistance to fatigue crack growth in adhesive bonds by measuring release of strain energy

Pascoe, John- Alan; Alderliesten, Rene; Benedictus, Rinze

DOI

[10.1016/j.prostr.2016.06.011](https://doi.org/10.1016/j.prostr.2016.06.011)

Publication date

2016

Document Version

Final published version

Published in

Procedia Structural Integrity

Citation (APA)

Pascoe, J. A., Alderliesten, R., & Benedictus, R. (2016). Characterising resistance to fatigue crack growth in adhesive bonds by measuring release of strain energy. In F. Iacoviello, L. Susmel, D. Firrao, & G. Ferro (Eds.), *Procedia Structural Integrity* (Vol. 2, pp. 80-87). Elsevier. <https://doi.org/10.1016/j.prostr.2016.06.011>

Important note

To cite this publication, please use the final published version (if applicable). Please check the document version above.

Copyright

Other than for strictly personal use, it is not permitted to download, forward or distribute the text or part of it, without the consent of the author(s) and/or copyright holder(s), unless the work is under an open content license such as Creative Commons.

Takedown policy

Please contact us and provide details if you believe this document breaches copyrights. We will remove access to the work immediately and investigate your claim.



21st European Conference on Fracture, ECF21, 20-24 June 2016, Catania, Italy

Characterising resistance to fatigue crack growth in adhesive bonds by measuring release of strain energy

J.A. Pascoe^{a,*}, R.C. Alderliesten^a, R. Benedictus^a

^aStructural Integrity & Composites, Faculty of Aerospace Engineering, Delft University of Technology, 2629 HS Delft, The Netherlands

Abstract

Measurement of the energy dissipation during fatigue crack growth is used as a technique to gain more insight into the physics of the crack growth process. It is shown that the amount of energy dissipation required per unit of crack growth is determined by G_{\max} , whereas the total amount of energy available for crack growth in a single cycle is determined by $(\Delta \sqrt{G})^2$.

© 2016, PROSTR (Procedia Structural Integrity) Hosting by Elsevier Ltd. All rights reserved.
Peer-review under responsibility of the Scientific Committee of PCF 2016.

Keywords: Adhesive Bonds; Fatigue Crack Growth; Strain Energy Dissipation

Nomenclature

a	Crack length	n	Calibration parameter
A	Fit parameter in the Jones model	P	Force
C	Curve fit parameter	R	Load ratio
d	Displacement	U	Strain energy
G	Strain energy release rate	w	Width
G_{th}	Threshold strain energy release rate	ΔG	Strain energy release rate range
K	Stress intensity factor	ΔK	Stress intensity factor range
N	Cycle number	γ	Mean stress sensitivity
n	Curve fit parameter		

* Corresponding author. Tel.: +31-15-2786604 ; fax: +31-15-2781151.
E-mail address: j.a.pascoe@tudelft.nl; johnalan.pascoe@gmail.com

1. Introduction

Since the pioneering work of Roderick et al. (1974) and Mostovoy and Ripling (1975), there have been many attempts to model fatigue crack growth (FCG) in composites and adhesive bonds. However these models are invariably based purely on empirical correlations (Pascoe et al., 2013). This is most likely because most research in this area has been focused on predicting crack growth, rather than gaining more understanding of the underlying physics.

The basis for most models dealing with FCG in composites and adhesives is the equation proposed in Paris (1964), but modified to depend on the strain energy release rate (SERR), G , rather than the stress intensity factor (SIF), K , i.e:

$$\frac{da}{dN} = C\Delta K^n \quad \text{or} \quad \frac{da}{dN} = CG_{\max}^n \quad \text{or} \quad \frac{da}{dN} = C\Delta G^n \quad (1)$$

where a is the crack length, N is the cycle number, and C and n are empirically determined curve fit parameters.

In the work of Paris et al. (1961) and Paris (1964) it was already noted that the crack growth rate depended not only on SIF range ΔK , but also on the ratio of minimum to maximum stress, R . Paris (1964) suggested that this could be accounted for by varying the coefficient C in equation 1 as a function of R .

Later researchers have suggested different ways of accounting for the R -ratio (or for the mean stress effect, which is equivalent). Hojo et al. (1987, 1994), Atodaria et al. (1997, 1999a,b), and Khan (2013) all proposed variations of the Paris equation, but with da/dN as a function of both G_{\max} and ΔG simultaneously. Allegri et al. (2011) proposed a power-law dependence of da/dN on G_{\max} , including R in the exponent. Andersons et al. (2004) and Jones et al. (2012, 2014a,b, 2016) have proposed modifications of the equation suggested by Priddle (1976) and Hartman and Schijve (1970).

A characteristic of all these models is that they are phenomenological. The form of the equations was not chosen based on principles of the physical behaviour of the material, but solely based on the shape of the graph of da/dN vs a chosen similitude parameter. Although this approach can result in good predictions, as long as there is sufficient experimental data available to calibrate the models, an actual understanding of fatigue crack growth remains lacking. This means very large tests campaigns are necessary to generate sufficient data, and that it is sometimes unclear what the limits of validity of the found correlations are.

The research presented in this paper aims to increase the understanding of FCG in adhesive bonds, rather than just creating yet another prediction model. To that end the strain energy dissipation during FCG in an adhesive joint was characterised, following the methodology established by Pascoe et al. (2014b, 2015).

2. Test set-up and data processing

FCG tests were performed on double cantilever beam (DCB) specimens, consisting of two aluminium 2024-T3 arms bonded with FM94 epoxy adhesive, cured according to the manufacturer's instructions. Adhesive tape was applied between the adhesive and the adherents to act as a crack starter. The nominal specimen width was 25 mm. For more details on specimen preparation see Pascoe et al. (2015). Actual dimensions for each specimen are available from the online dataset (Pascoe et al., 2014a).

Tests were performed on an MTS 10 kN fatigue machine under displacement control, at a frequency of 5 Hz. Before each fatigue test the specimens were loaded quasi-statically until onset of crack growth was determined visually. Table 1 shows the applied load ratios for the experiments discussed here. For convenience of presentation the experiments have been collected into 4 groups according to applied R -ratio, as is also shown in table 1.

The crack length was measured by means of a camera aimed at the side of the specimen. Photographs were taken at regular intervals (once every 100 cycles at the start of the test, after approximately 10,000 cycles this was increased to once every 1,000 cycles) while the specimen was held at the maximum displacement. After completion of the test, an image recognition algorithm was used to automatically determine the crack length in each picture. A power-law curve was then fit through the crack length vs cycle number data. The crack growth rate was determined by taking the derivative of this power-law.

Table 1. Applied load ratios in terms of $R_p = P_{\min}/P_{\max}$ and $R_d = d_{\min}/d_{\max}$.

Specimen	Mean R_d	Standard deviation R_d	Mean R_p	Standard deviation R_p	Group
B-001-II	0.10	$4.0 \cdot 10^{-4}$	0.036	0.0060	$R = 0.036$
E-002-I	$2.3 \cdot 10^{-4}$	$6.3 \cdot 10^{-4}$	-0.022	0.0056	$R = 0.036$
E-002-II	$-9.3 \cdot 10^{-5}$	$4.5 \cdot 10^{-4}$	0.014	0.0047	$R = 0.036$
C-001-I	0.33	0.0010	0.29	0.0047	$R = 0.29$
D-002	0.29	$2.8597 \cdot 10^{-4}$	0.29	0.0017	$R = 0.29$
E-001-I	0.29	0.012	0.24	0.012	$R = 0.29$
E-001-II	0.29	$3.6 \cdot 10^{-4}$	0.27	0.0021	$R = 0.29$
B-002-II	0.74	$3.5 \cdot 10^{-4}$	0.61	0.015	$R = 0.61$
C-002-D	0.67	0.0087	0.61	0.010	$R = 0.61$
E-003-I	0.61	$7.6 \cdot 10^{-4}$	0.60	0.0029	$R = 0.61$
E-003-II	0.61	$3.94 \cdot 10^{-4}$	0.62	0.0027	$R = 0.61$
B-002-I	0.88	$4.6 \cdot 10^{-4}$	0.86	0.0015	$R = 0.86$

The maximum and minimum force and displacement were recorded by the test machine every 100 cycles. From this the SERR was determined using the compliance calibration method described in ASTM Standard D 5528/ D 5528-01, 2007 (2007).

$$G = \frac{nPd}{2wa} \quad (2)$$

where P is the force, d is the displacement, w is the specimen width, a is the crack length, and n is a calibration parameter, which was determined individually for each experiment.

The force and the displacement was also used to calculate the strain energy in the specimen, following the methodology of Pascoe et al. (2014b, 2015):

$$U_{\text{tot}} = \frac{1}{2} P_{\max} (d_{\max} - d_0) \quad (3)$$

$$U_{\text{cyc}} = \frac{1}{2} P_{\max} (d_{\max} - d_0) - \frac{1}{2} P_{\min} (d_{\min} - d_0) \quad (4)$$

where U_{tot} is the total strain energy in the system, U_{cyc} is the cyclic work which is applied during a load cycle, and d_0 is the displacement for which the force is 0. A power-law curve was fit through the U vs N data for each experiment. The derivative of this power law was used to find the energy dissipation per cycle dU/dN . These definitions and the process used to determine dU/dN are shown in figure 1

3. Results

First the crack growth rate has been plotted against similitude parameters based on linear elastic fracture mechanics (LEFM), as is the traditional approach. Figure 2 shows the crack growth rate as a function of G_{\max} and $(\Delta \sqrt{G})^2 = (\sqrt{G_{\max}} - \sqrt{G_{\min}})^2$. This second parameter has recently been suggested as the appropriate similitude parameter by Rans et al. (2011) and Jones et al. (2016) and is equivalent to ΔK .

For both G_{\max} and $(\Delta \sqrt{G})^2$ there is a clear R -ratio effect, in accordance with what is usually reported in literature. That there is an R -ratio effect should not be surprising: for a given G_{\max} , an increase in R -ratio implies a decrease in

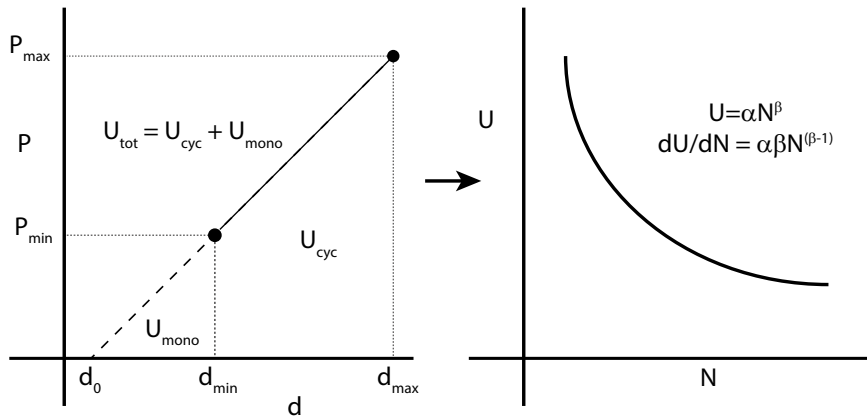


Fig. 1. Definition of the various terms related to the strain energy and a schematic example of how dU/dN was determined. From the measured load and displacement, U was determined. A curve fit was then used to find a function relating U to N . dU/dN follows from the derivative of this function.

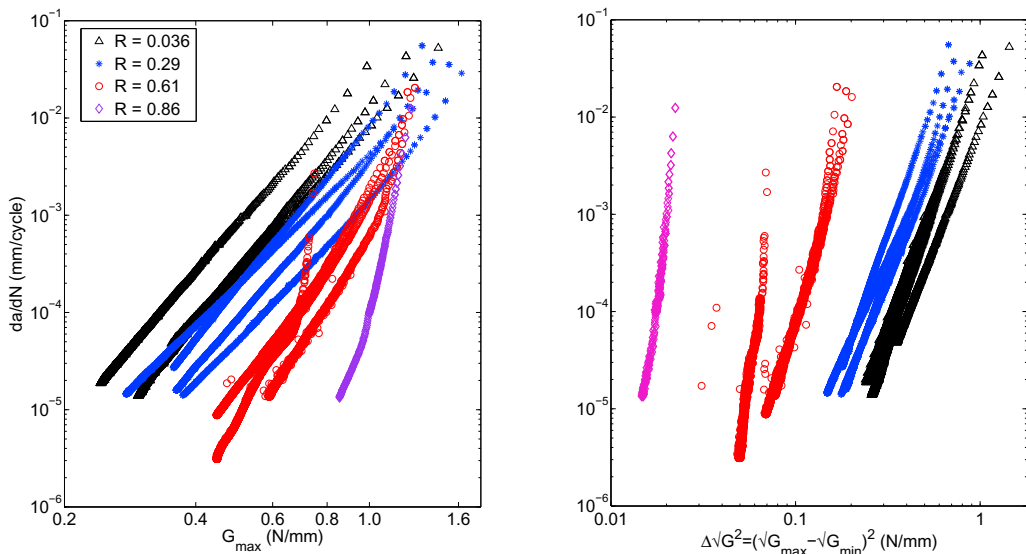


Fig. 2. da/dN as a function of G_{max} (left) and $(\Delta \sqrt{G})^2$ (right).

$(\Delta \sqrt{G})^2$ (or ΔG), and thus a decrease in da/dN would also be expected, and is indeed seen here. Likewise, for a given $(\Delta \sqrt{G})^2$ an increase in R -ratio implies an increase in G_{max} (or mean load), and therefore the increase in da/dN that is seen should be expected.

Figure 3 shows the crack growth rate as a function of the energy dissipation per cycle (dU/dN). It is clear that there is a very strong correlation, and with the exception of one outlier, the curves for the different experiments appear to collapse onto one line. In fact there is still a small R -ratio effect present, which will be discussed below. First however,

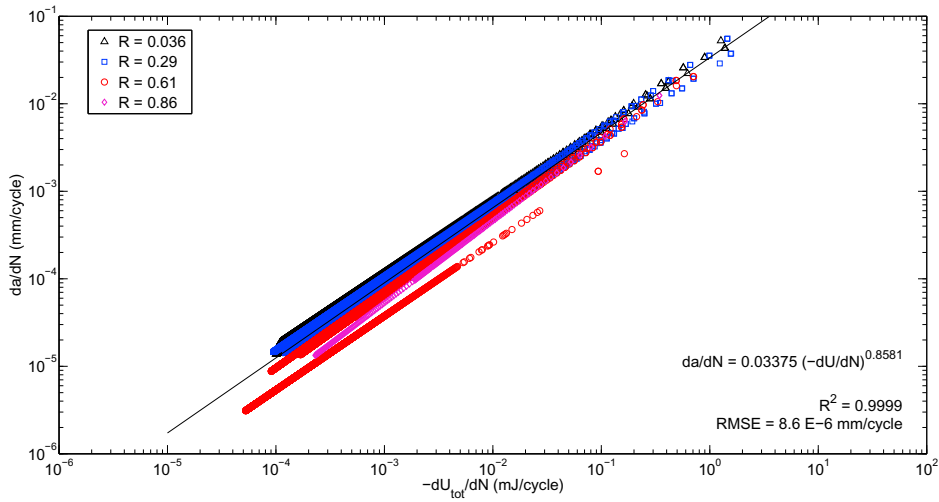


Fig. 3. da/dN as a function of dU_{tot}/dN .

it should be noted that the correlation between da/dN and dU/dN can be captured by a power-law relationship, i.e.

$$\frac{da}{dN} = C \left(-\frac{dU}{dN} \right)^n \quad (5)$$

with an exponent $n \approx 0.86$. This implies that the amount of energy dissipation per unit of crack growth is not constant. At higher crack growth rates the amount of energy dissipated per unit of crack growth is higher. For example, if the amount of energy dissipation in a cycle is increased by a factor of 2, the amount of crack growth in that cycle will only increase by a factor of 1.8.

At this point it is convenient to introduce a notation for the energy dissipated per unit of crack growth: G^* , defined as (Pascoe et al., 2014b, 2015):

$$G^* = \frac{-\frac{dU}{dN}}{w \frac{da}{dN}} \quad (6)$$

G^* is thus a kind of average SERR during a single fatigue cycle. However it should be noted that G^* is not in general equal to the mean of the applied G cycle.

The data presented in figure 3 imply that at higher crack growth rates G^* is also higher. However, G^* is not only correlated to the crack growth rate, but also to the applied load. This can be clearly seen in figure 4, which shows the energy dissipation (dU/dN) as a function of G_{max} , and $(\Delta \sqrt{G})^2$, for a fixed crack growth rate value of 10^{-4} mm/cycle. As the crack growth rate is the same for all these data points, each dU/dN value corresponds directly to a specific G^* (energy dissipation per unit of crack growth) value.

It is clear that the amount of energy dissipated in order to produce this amount of crack growth was not the same in each experiment. The maximum amount of energy required to produce 10^{-4} mm of crack growth is a factor of 2.4 higher than the minimum required amount. Likewise there is a wide range of G_{max} values that can all result in a crack growth rate of 10^{-4} mm/cycle. There is also a clear linear relationship between G_{max} and dU/dN (and therefore G^*). The higher G_{max} (and R), the more energy was dissipated per unit of crack growth. This implies that at higher

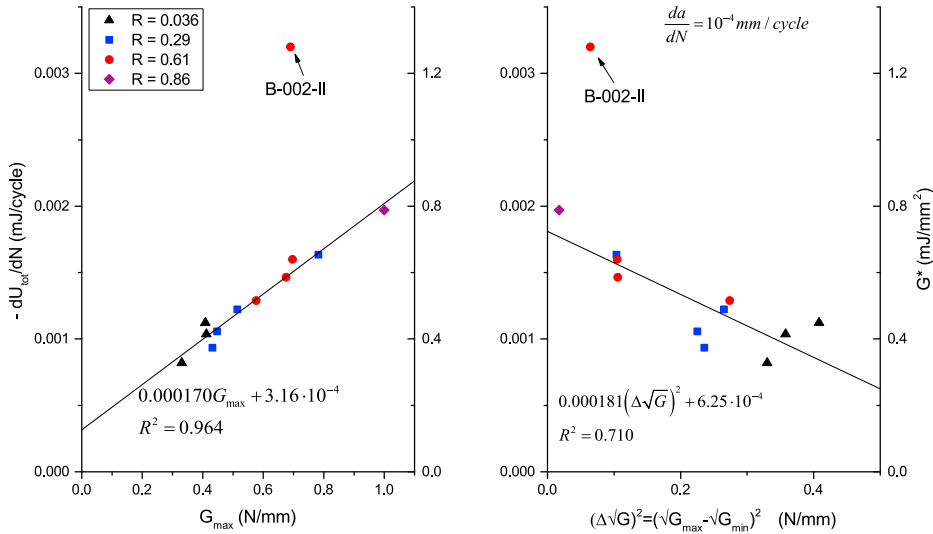


Fig. 4. Energy dissipation at a crack growth rate of 10^{-4} mm/cycle as a function of G_{max} (left panel) and $(\Delta \sqrt{G})^2$ (right panel). Note that the graphs are not independent: a crack growth rate of 10^{-4} mm/cycle only occurs for specific combinations of G_{max} and $(\Delta \sqrt{G})^2$, so a higher value of G_{max} in the left panel implies a lower matching value of $(\Delta \sqrt{G})^2$ in the right panel, and vice versa. Linear fits through the data points are also shown. The data for experiment B-002-II was excluded from these fits as an outlier. As all data points in this figure correspond to the same da/dN value, an approximation of G^* is also shown, obtained by dividing the axis values by $25 \cdot 10^{-4}$.

G_{max} values, a greater fraction of the energy dissipation is caused by mechanisms that do not directly contribute to the crack growth. In other words, at higher G_{max} values, the resistance to crack growth is greater; more energy needs to be dissipated for the same amount of crack growth.

For the experiments shown in figure 4 the resistance is different for each experiment, yet the crack growth rate is the same. Therefore there must be a second parameter that controls the crack growth rate. Rewriting equation 6 one obtains:

$$\frac{da}{dN} = -\frac{1}{wG^*} \frac{dU}{dN} \tag{7}$$

Therefore if G^* is fixed, the crack growth rate must be controlled by dU/dN . The measured dU/dN is the energy dissipation. However, by the first law of thermodynamics this must also equal the total amount of energy available for crack growth. Thus the amount of crack growth in a cycle is equal to the available energy divided by the amount of energy required per unit of crack growth, which makes sense.

Figure 5 shows dU/dN as a function of $(\Delta \sqrt{G})^2$ and U_{cyc} for a given G^* value. There is a clear correlation between dU/dN and both $(\Delta \sqrt{G})^2$, and U_{cyc} . Thus if G^* is given, dU/dN is determined by $(\Delta \sqrt{G})^2$ or U_{cyc} . It should be noted that the relationships are non-linear. E.g. increasing U_{cyc} by a factor of 2 will increase the energy dissipation by a factor of 12. This implies that for higher U_{cyc} and $(\Delta \sqrt{G})^2$ values, not only is more energy being put into the system, on top of that a larger fraction of that energy is available for crack growth. I.e. both the absolute value of dU/dN , and the ratio of dU/dN to U_{cyc} will increase.

4. Discussion

Putting the above together, the following model of fatigue crack growth can be formulated: The amount of crack growth in a cycle is determined by the total energy dissipation, dU/dN , divided by the energy dissipation per unit of

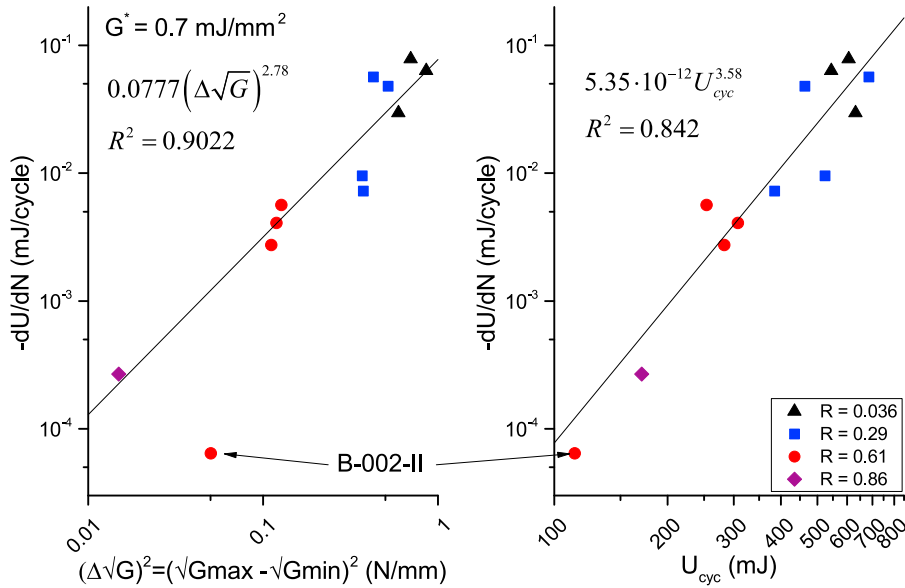


Fig. 5. dU/dN as a function of $(\Delta \sqrt{G})^2$ (left panel) and U_{cyc} (right panel) for a fixed value of $G^* = 0.7 \text{ mJ/mm}^2$. Power-law curve fits are also shown. To produce these fits, B-002-II was excluded as an outlier. Note that since G^* is fixed, each value of dU/dN corresponds directly to a single da/dN value.

crack growth, G^* . Thus dU/dN is a measure of the total energy available for crack growth, and G^* is a measure of the resistance to crack growth. If dU/dN is increased (and all other parameters are kept the same) the crack growth rate will increase, whereas if G^* is increased, the crack growth rate will decrease.

It is clear that both dU/dN and G^* depend on the applied load. In particular G^* is correlated to G_{max} , and dU/dN is correlated to $(\Delta \sqrt{G})^2$. Why these relationships exist is not entirely clear, but some preliminary hypotheses can be sketched. In the vicinity of the crack tip there will be plastic deformation. This dissipates energy without contributing to crack growth. Therefore more plastic deformation means more energy dissipation per unit of crack growth. The amount of plastic deformation depends on G_{max} . Thus if G_{max} is higher, there will be more plastic deformation, and therefore more energy dissipation per unit of crack growth, i.e. G^* will be higher.

On the other hand, U_{cyc} and $(\Delta \sqrt{G})^2$ represent the work performed on a specimen by the loading device during a fatigue cycle. That an increase in work done on the specimen also leads to an increase in the amount of energy available for crack growth is logical. Why the relationship is non-linear will have to be studied further.

5. Conclusion

In order to gain more insight into the physical processes underlying fatigue crack growth, the energy dissipation during fatigue crack growth was measured in an adhesive bond. It was shown that the crack growth rate is strongly correlated to the energy dissipation per cycle. It was also shown that the amount of energy dissipation per unit of crack growth, G^* , is strongly correlated to G_{max} . G^* can be interpreted as the resistance to fatigue crack growth.

The crack growth rate depends not only on the resistance to crack growth, but also on the amount of energy available for crack growth, which was shown to correlate to the applied cyclic work U_{cyc} and the cyclic SERR parameter $(\Delta \sqrt{G})^2$.

These results show that models of FCG should take both G_{max} and $(\Delta \sqrt{G})^2$ in to account, and that using only one of these parameters is insufficient. Some hints as to the physical meaning of these parameters were uncovered. The

next step for future research is to explain how the applied load influences the available energy for crack growth, and the fatigue crack growth resistance.

Acknowledgements

This research was made possible by a grant from the Netherlands Organisation for Scientific Research (NWO) Mosaic programme under project number 017.009.005.

References

- Allegrì, G., Jones, M.I., Wisnom, M.R., Hallett, S.R., 2011. A new semi-empirical model for stress ratio effect on mode II fatigue delamination growth. *Composites Part A* 42, 733–740.
- Andersson, J., Hojo, M., Ochiai, S., 2004. Empirical model for stress ratio effect on fatigue delamination growth rate in composite laminates. *Int J Fatigue* 26, 597–604.
- ASTM Standard D 5528/ D 5528-01, 2007, 2007. Standard test method for mode I interlaminar fracture toughness of unidirectional fiber-reinforced polymer matrix composites. ASTM International, West Conshohocken, PA, USA.
- Atodaria, D.R., Putatunda, S.K., Mallick, P.K., 1997. A fatigue crack growth model for random fiber composites. *J Compos Mater* 31, 1838–1855.
- Atodaria, D.R., Putatunda, S.K., Mallick, P.K., 1999a. Delamination growth behavior of a fabric reinforced laminated composite under mode I fatigue. *J Eng Mater Technol* 121, 381–385.
- Atodaria, D.R., Putatunda, S.K., Mallick, P.K., 1999b. Fatigue crack growth model and mechanism of a random fiber SMC composite. *Polym Compos* 20, 240–249.
- Hartman, A., Schijve, J., 1970. The effects of environment and load frequency on the crack propagation law for macro fatigue crack growth in aluminium alloys. *Eng Fract Mech* 1, 615–631.
- Hojo, M., Ochiai, S., Gustafson, C.G., Tanaka, K., 1994. Effect of matrix resin on delamination fatigue crack growth in CFRP laminates. *Eng Fract Mech* 49, 35–47.
- Hojo, M., Tanaka, K., Gustafson, C.G., Hayashi, R., 1987. Effect of stress ratio on near-threshold propagation of delamination fatigue cracks in unidirectional CFRP. *Compos Sci Technol* 29, 273–292.
- Jones, R., Hu, W., Kinloch, A.J., 2014a. A convenient way to represent fatigue crack growth in structural adhesives. *Fatigue & Fracture of Engineering Materials & Structures* 38, 379–391.
- Jones, R., Kinloch, A.J., Hu, W., 2016. Cyclic-fatigue crack growth in composite and adhesively-bonded structures: The faa slow crack growth approach to certification and the problem of similitude. *Int J Fatigue* 88, 10–18.
- Jones, R., Pitt, S., Bunner, A.J., Hui, D., 2012. Application of the Hartman-Schijve equation to represent mode I and mode II fatigue delamination growth in composites. *Compos Struct* 94, 1343–1351.
- Jones, R., Stelzer, S., Brunner, A.J., 2014b. Mode I, II and mixed mode I/II delamination growth in composites. *Compos Struct* 110, 317–324.
- Khan, R., 2013. Mode I Fatigue delamination growth in composites. Phd thesis. Delft University of Technology.
- Mostovoy, S., Ripling, E., 1975. *Flaw Tolerance of a Number of Commercial and Experimental Adhesives*. Plenum Press, New York. *Polymer Science and Technology* 9B, pp. 513–562.
- Paris, P., 1964. The fracture mechanics approach to fatigue, in: 10th Sagamore Army Materials Research Conference, Syracuse University Press. pp. 107–132.
- Paris, P., Gomez, M., Anderson, W., 1961. A rational analytic theory of fatigue. *The Trend in Engineering* 13, 9–14.
- Pascoe, J.A., Alderliesten, R.C., Benedictus, R., 2013. Methods for the prediction of fatigue delamination growth in composites and adhesive bonds - a critical review. *Eng Fract Mech* 112–113, 72–96.
- Pascoe, J.A., Alderliesten, R.C., Benedictus, R., 2014a. Damage tolerance of adhesive bonds - datasets. Collection of datasets, available at: <http://dx.doi.org/10.4121/uuid:c43549b8-606e-4540-b75e-235b1e29f81d>.
- Pascoe, J.A., Alderliesten, R.C., Benedictus, R., 2014b. Towards understanding fatigue disbond growth via cyclic strain energy. *Procedia Materials Science* 3 (ECF-20), 610–615.
- Pascoe, J.A., Alderliesten, R.C., Benedictus, R., 2015. On the relationship between disbond growth and the release of strain energy. *Eng Fract Mech* 133, 1–13.
- Priddle, E., 1976. High cycle fatigue crack propagation under random and constant amplitude loadings. *International Journal of Pressure Vessels and Piping* 4, 89–117.
- Rans, C., Alderliesten, R.C., Benedictus, R., 2011. Misinterpreting the results: How similitude can improve our understanding of fatigue delamination growth. *Compos Sci Technol* 71, 230–238.
- Roderick, G., Everett, R., Crews Jr, J., 1974. *Debond Propagation in Composite Reinforced Metals*. Technical Report NASA TM X-71948. NASA.